

## Photoemission above the Fermi Level: The Top of the Minority $d$ Band in Nickel

T. Greber, T. J. Kreutz, and J. Osterwalder

*Physik-Institut, Universität Zürich-Irchel, Winterthurerstrasse 190, CH-8057 Zürich, Switzerland*

(Received 2 July 1997)

The magnetic phase transition in nickel metal has been studied with high resolution photoemission spectroscopy. A monochromatized high intensity He  $I\alpha$  photon source provides access to the dispersion of thermally populated states up to  $5k_B T$  above the Fermi level. On Ni(111) the coalescence of the partially occupied minority  $d$  band and the occupied majority  $d$  band is observed in raising the temperature above the Curie point. Close to a fast dispersing  $sp$  band anomalously high intensity from the minority  $d$  band is found. This is a clue that  $sp-d$  fluctuations at the Fermi level are a driving force in the magnetic phase transition. [S0031-9007(97)04631-0]

PACS numbers: 75.25.+z, 71.18.+y, 75.10.Lp, 79.60.Bm

Nickel metal is a prototypical itinerant ferromagnet. Over the years, many experimental signatures of the ferromagnetic-to-paramagnetic phase transition have accumulated, which have proven difficult to be described by one consistent theory [1]: Neutron scattering experiments find local moments and spin waves above the Curie temperature ( $T_c$ ) [2]. Angle-resolved photoemission and inverse photoemission (IPE) emphasize the itinerant nature of the electronic states and see a Stoner-like collapse of the exchange splitting  $\Delta\epsilon_{ex}$  [3,4], with the exception of two spin-polarized photoemission studies involving the resonant excitation of core holes in the valence photoemission process. These experiments give evidence for persisting local moments in the paramagnetic state [5,6].

Theories combining local and itinerant aspects include local-band theories [1,7–9] involving considerable short-range magnetic order above  $T_c$  and a recent generalized Hubbard model which produces the full temperature dependence of the quasiparticle band structure [10]. Specific signatures of these theories have been looked for in recent photoemission experiments. A spin- and angle-resolved photoemission study, looking at the details of the spin-dependent band structure, found locations in  $k$  space where the separation  $\Delta\epsilon_{ex}$  of spin-pairs of bands remains temperature independent, while at other locations a collapse was observed when  $T_c$  was approached from below [11]. Likewise, in a Fermi surface mapping experiment using high-resolution spin-integrated angle-resolved photoemission, large portions of the Fermi surface reflected a collapsing exchange splitting, while some parts appeared to remain stationary with temperature [12].

In this paper we address this issue specifically by looking more closely at those regions in  $k$  space where the minority  $d$  band crosses the Fermi level ( $\epsilon_F$ ). Any temperature-dependent shift of this band is related to a change in the minority spin occupation number  $n_d$ , and thus the magnetically active part of the band structure is measured. For this purpose we have extended the energy range covered by angle-resolved photoemission to slightly above  $\epsilon_F$  such as to follow the dispersion of the thermally

excited top of the minority  $d$  band. This procedure, which is described in the next paragraph, enables us to monitor the temperature dependence of a complete spin-pair of a magnetic  $d$  band in one single experiment rather than by combining information from direct and inverse photoemission data.

Near the Fermi energy, the measurement of electronic states by photoemission is compromised by the changes in occupation numbers associated with the Fermi-Dirac (FD) distribution function. Except for a few studies [13,14], the extremely rapid falloff of the FD function has so far discouraged people from trying to recover spectral features in the tail of thermally excited electrons. In order to detect significant spectral contributions in this interesting energy range, two conditions must be met: (i) A clean and highly intensive photon source must provide low background intensities above  $\epsilon_F$ , and (ii) the experimental energy resolution must be at least of the order of the temperature broadening.

We have met these conditions in an improved experimental setup which is based on a VG ESCALAB 220 spectrometer with an ultimate energy resolution of 20 meV and an angular resolution below  $1^\circ$ . The sample goniometer permitting high precision control of polar and azimuthal angles has been described elsewhere [15]. For excitation we use a microwave-driven high flux He discharge lamp in combination with a toroidal grating monochromator (Gammadata Burklint AB, Sweden). The monochromatized light intensity on the sample is  $5 \times 10^{12}$  photons/sec for He  $I\alpha$  radiation (21.2 eV) on a 3 mm spot. Higher energy He radiation is suppressed from 11% in zero order diffraction by more than a factor of 50 in first order. The photon flux is very stable over a long period of time, which is crucial for the type of data sets described below where spectra measured over a series of polar angles are normalized energy channel by energy channel.

In Fig. 1 we present spectra measured on a polycrystalline Ag sample, using zero order and first order He  $I\alpha$  radiation. The logarithmic representation (lower panel)

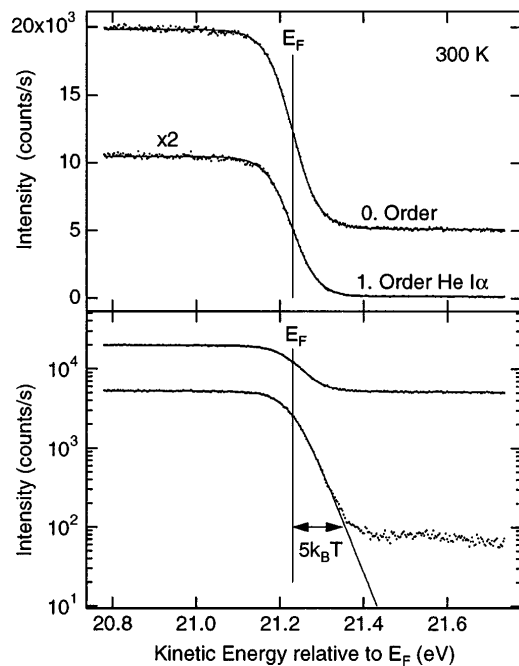


FIG. 1. Photoemission spectra taken near the Fermi level from polycrystalline Ag at 300 K. The analyzer energy resolution was 35 meV, and unmonochromatized (zero order) and monochromatized (1st order) He  $I\alpha$  radiation was used for excitation. In the lower panel a logarithmic intensity scale has been chosen for the same data.

illustrates that, for monochromatized He  $I\alpha$  excitation, the Boltzmann tail of the FD function is drowned by the background intensity at  $5k_B T$  above the Fermi energy. Inside this extra range meaningful information can still be extracted from our photoemission data.

An important consistency check for the validity of observed features above  $\epsilon_F$  is furthermore provided by the following procedure: Our highly accurate and automated mode of collecting photoemission data both as a function of energy and emission angle [16] produces two-dimensional data sets of the kind shown in Fig. 2. Energy distribution curves (EDCs) have been measured from a clean Ni(111) surface, covering binding energies from  $-2.0$  to  $+1.6$  eV and a contiguous range of polar angles along a particular sample azimuth (see below). In Fig. 2(a), raw intensity data are displayed in a linear gray scale, exhibiting the sharp FD cutoff. In Fig. 2(b), the data have been normalized such as to produce maximum angular contrast along each horizontal line, i.e., for each energy the minimum intensity is assigned black and the maximum intensity white. For energies above  $\epsilon_F$ , well-defined structures become visible in the normalized data. The upper inverted parabolic band near  $\epsilon_F$  now exhibits its apex near  $40^\circ$  polar angle. Further replicas of these parabolas appear at higher energies due to remnant satellite lines in the photon spectrum (C III and He I  $\beta$ ).

The data of Fig. 2 represent a polar scan of EDCs on the (111) surface of Ni along the azimuth which is  $67^\circ$  off

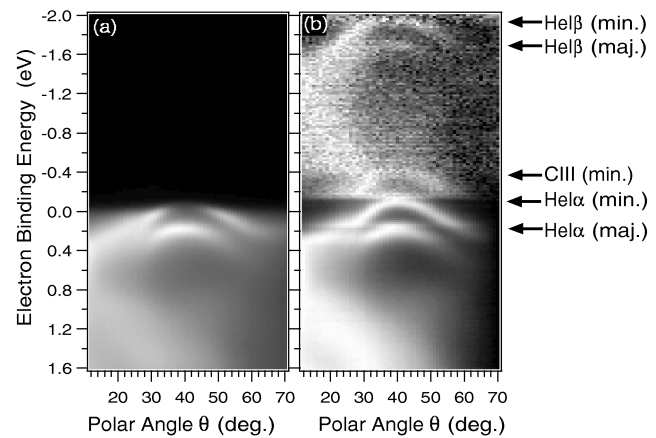


FIG. 2. Angle-scanned EDCs from Ni(111) measured with He  $I\alpha$  radiation. In (a) the raw data are shown, while in (b) the data have been normalized for maximal angular contrast. The linear gray scale ranges from black at minimum intensity to white at maximum intensity.

the  $[\bar{1}10]$  direction and  $23^\circ$  off  $[\bar{1}\bar{1}2]$ . We have selected this particular region in  $k$  space because this is where the magnetic  $d$  band crosses the Fermi level. In relation to the Fermi surface contours measured by Aebi *et al.* [see Fig. 1(a) of Ref. [12]], our polar scan represents a section containing the features A and B [12]. In Figs. 3(b), 3(c), and 3(d) we show the temperature dependence of these photoemission data near  $\epsilon_F$  measured from the surface normal to  $72^\circ$  off normal. Differing from the procedure applied in Fig. 2(b), the data have here been normalized by the FD function convoluted with the experimental resolution [17] (cf. the Figure caption), and then plotted in a linear gray scale.

In the room temperature data [Fig. 3(b)] we can clearly resolve two inverted parabolic bands with their apexes located at  $40^\circ$ . Band structure calculations using the spin-polarized Layer-Korringa-Kohn-Rostoker (LKKR) [18] formalism have been performed for the same region in  $k$  space [Fig. 3(a)]. The agreement between the calculated bands and the band features in Fig. 3(b) is remarkable except for a renormalization of the energy scale due to self-energy effects in the photohole state. The upper parabola can be identified with the top of the minority  $d$  band while the lower one represents the fully occupied majority twin [19].

From the normalized data near the apex position [Figs. 3(b) and Fig. 4], a value of  $280 \pm 20$  meV for the exchange splitting at room temperature can be extracted, which is in beautiful agreement with a recent inverse photoemission study along the Z line [3]. Using a maximum-entropy regularization to deconvolute the spin-polarized IPE spectra, spin-dependent quasiparticle spectral densities were obtained, indicating an extrapolated groundstate exchange splitting of  $280 \pm 50$  meV [3]. Notice that we have extracted the room temperature value, which is already close to saturation, essentially from the raw data.

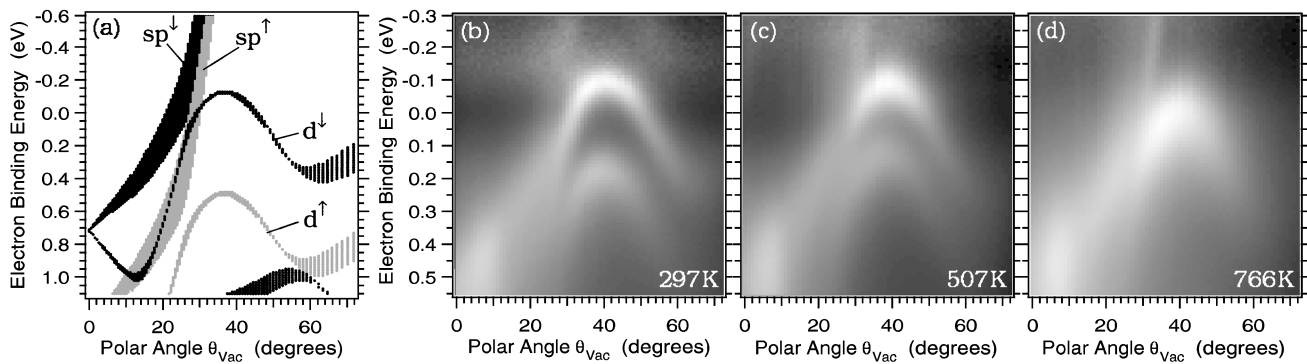


FIG. 3. (a) Spin-polarized LKKR calculation covering the section in  $\vec{k}$  space of our measurements. Majority spin bands are given in gray, minority bands in black. (b)–(d): He  $I\alpha$  excited polar-angle scanned EDCs taken from Ni(111) along the azimuth which is  $67^\circ$  off the  $[110]$  direction and  $23^\circ$  off  $[112]$ , measured at three different temperatures: (b)  $0.47T_c$ , (c)  $0.80T_c$ , and (d)  $1.21T_c$ . All spectra have been normalized by a Fermi-Dirac distribution function which rides on a small constant background in order to avoid zero divisions. The linear gray scale ranges from minimum (black) to maximum (white) intensity.

Figures 3(c) and 3(d) present data measured along the same  $\vec{k}$  space sections for temperatures of  $0.80T_c$  and  $1.21T_c$ , respectively. The collapse of the exchange splitting between the  $d^\uparrow$  and  $d^\downarrow$  bands is evident. Above  $T_c$  the two parabolas have coalesced very close to  $\epsilon_F$  and with now one common apex at  $\theta = 40^\circ$ . These data thus confirm the Stoner-type behavior of the magnetic  $d$  band as has been inferred from the spin-polarized IPE data [3]. The presence of clearly dispersing bands in the elevated-temperature data indicate that the influence due to phonon-assisted nondirect transitions [20] is weak.

The LKKR calculation produces another pair of bands,  $sp^\downarrow$  and  $sp^\uparrow$ , which both cross the Fermi energy at nearly the same position as the minority  $d^\downarrow$  band near

$\theta = 28^\circ$ . These bands are clearly resolved at high temperatures. In these data the measuring range is expanded from  $5kT = 130$  meV (RT) to 220 meV ( $0.80T_c$ ) and 330 meV ( $1.21T_c$ ). The combination of the increased thermal population of excited states and the shift of the minority  $d$  band towards  $\epsilon_F$  leads to a situation where the  $sp$  bands are clearly exposed and appear as a very fast dispersing feature crossing the Fermi level near  $\theta = 30^\circ$ . Because of the close spacing between the  $sp^\downarrow$  and  $sp^\uparrow$  bands in this  $\vec{k}$  region [Fig. 3(a)] we cannot resolve the individual components. The dispersion is too fast for observing the exchange splitting in a spin-integrated experiment: The slope of the measured feature is 125 meV per degree, and a value of  $\Delta\epsilon_{ex} = 200$  meV for the  $sp$  band [16] would reflect itself in an angular separation of  $1.6^\circ$  which is less than the width of the observed feature. This pair of  $sp$  bands thus appears stationary with temperature even for a Stoner-type collapse of  $\Delta\epsilon_{ex}$ . Since the examined location in  $\vec{k}$  space is equivalent to that of the stationary Fermi-surface contours on Ni(110) [12], we have found a natural explanation for this observation which is fully consistent with the Stoner picture.

Figure 4 shows EDCs extracted from the Fermi-Dirac-normalized data of Figs. 3(b)–3(d) at the apex of the  $d$  bands. The enhanced intensity from the minority  $d$  band relative to the majority  $d$  band below  $T_c$  is most striking. This is not an artifact of the normalization procedure, and we obtain quantitatively the same results by normalizing the energy spectra with the average intensity on each polar scan. The intensity difference is unlikely to be caused by matrix element effects because of the close proximity of the bands in energy and in  $\vec{k}$  space. A spin-dependent matrix element effect is ruled out by our experimental setup, since the average sample magnetization is zero and weakly linearly polarized light is used. We therefore interpret the high intensity of the emission from the minority  $d$  band to be caused by the interaction with the nearby  $sp$  band (see below).

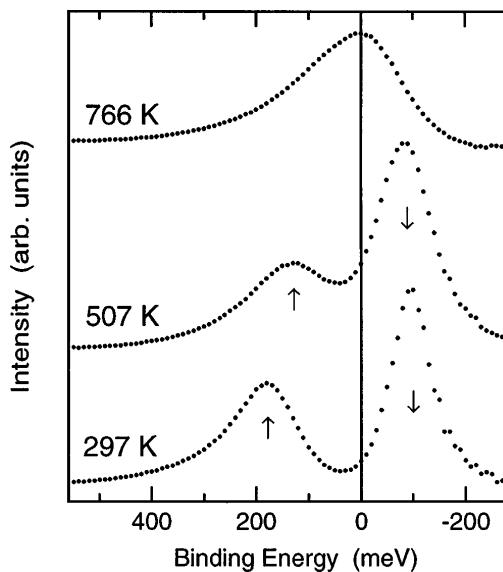


FIG. 4. EDCs extracted from the normalized data of Fig. 3(b)–3(d) at the apex of the  $d$  bands ( $\theta = 40^\circ$ ). Spin labels are indicated by the arrows. The curves are drawn with intensity offsets.

Thus the data sets of Figs. 3 and 4 provide two significant new aspects concerning the magnetic phase transition in Ni:

(1) We have identified a region in  $\vec{k}$  space where the minority  $d$  band and the two  $sp$  bands cross the Fermi level at the same  $\vec{k}$  and with nearly the same group velocity. The existence of such a configuration has important implications for the single-particle excitation spectrum. The Stoner gap, normally associated with spin-flip transitions  $d^\uparrow \rightarrow d^\downarrow$ , may here be reduced to zero, because transitions of the type  $sp^\uparrow \rightarrow d^\downarrow$  can be strong. In this scenario, the  $sp$  band acts as a minority-spin electron reservoir, permitting  $d^\downarrow$  states to be filled before the  $d^\uparrow$  band starts being depopulated upon raising the temperature. The related reduction of the average magnetic moment, and thus of  $\Delta\epsilon_{\text{ex}}$  supplies the positive feedback which drives the phase transition. The high intensity found for the minority  $d$  band apex at  $0.8T_c$  (Fig. 4, 507 K) supports this scenario: The interplay between the strong  $sp^\uparrow \rightarrow d^\downarrow$  scattering and the decreasing exchange splitting might pump more electrons into the  $d^\downarrow$  apex than one would have from the FD-type thermal population of a stationary band structure [21].

(2) A further indication that we have located the magnetically active region which drives the phase transition is that, above  $T_c$ , the top of the coalesced  $d$  band is found to lie precisely at the Fermi level [Fig. 4(d)]. This means that for this  $\vec{k}$  vector the creation of a spin flip costs no energy. Fluctuating local moments and spin waves in the paramagnetic phase are thus fully consistent with our measurements. Indeed, the anomalously large width observed for the normalized spectrum above  $T_c$  (Fig. 4) might be a consequence of these fluctuations [22].

In summary, the data of Fig. 3 represent a particularly striking demonstration of the enhanced sensitivity to band dispersion near and above  $\epsilon_F$  of this new photoemission mode. The occupied top of the majority  $d$  band and the unoccupied top of its minority twin can be monitored in one single spectrum with high-resolution photoemission, and their behavior can thus be studied as a function of temperature in unprecedented detail. As a result, we find that the previous observation of stationary features on the Fermi surface [12], which we fully reproduce, can be well explained by the presence of  $sp$  bands with high group velocities, and that the temperature behavior of all observed bands is of the Stoner type. We are convinced that this coincidence of  $sp$  and  $d$  electrons at the same location on the Fermi surface is highly important for driving the magnetic phase transition and we have observed similar situations in other regions of  $\vec{k}$  space.

We thank E. Wetli, P. Schwaller, F. Bourqui, and P. Soland for their assistance with the experiment and are obliged to P. Aebi who shared his modified LKKR code. Interesting discussions with M. Donath, D. Pescia, and R. Willis are gratefully acknowledged. This work was supported by the Swiss National Science Foundation.

- 
- [1] H. Capellmann, *Metallic Magnetism* (Springer, Berlin, 1987).
  - [2] G. Shirane, O. Steinsvoll, Y.J. Uemura, and J. Wicksted, *J. Appl. Phys.* **55**, 1887 (1984).
  - [3] W. von der Linden, M. Donath, and V. Dose, *Phys. Rev. Lett.* **71**, 899 (1993).
  - [4] M. Donath, *Surf. Sci. Rep.* **20**, 251 (1994).
  - [5] A. Kakizaki *et al.*, *Phys. Rev. Lett.* **72**, 2781 (1994).
  - [6] B. Sinkovic *et al.*, *Phys. Rev. Lett.* (to be published).
  - [7] H. Capellmann, *Z. Phys. B* **34**, 29 (1979).
  - [8] V. Korenman and R.E. Prange, *Phys. Rev. Lett.* **44**, 1291 (1980).
  - [9] V. Korenman and R.E. Prange, *Phys. Rev. Lett.* **53**, 186 (1984).
  - [10] W. Nolting, W. Borgiel, V. Dose, and T. Fauster, *Phys. Rev. B* **40**, 5015 (1989).
  - [11] K.-P. Kämper, W. Schmitt, and G. Güntherodt, *Phys. Rev. B* **42**, 10 696 (1990).
  - [12] P. Aebi *et al.*, *Phys. Rev. Lett.* **76**, 1150 (1996).
  - [13] E. Kisker, E.F. Wassermann, and C. Carbone, *Phys. Rev. Lett.* **58**, 1784 (1987).
  - [14] W.G. Park *et al.*, *Solid State Commun.* **91**, 655 (1994).
  - [15] J. Osterwalder, T. Greber, A. Stuck, and L. Schlapbach, *Phys. Rev. B* **44**, 13 764 (1991).
  - [16] T.J. Kreutz, P. Aebi, and J. Osterwalder, *Solid State Commun.* **96**, 339 (1995).
  - [17] Numerical simulations have shown that the convolution of the Fermi edge with the experimental resolution function, represented by a Gaussian with a full width at half maximum of  $\Delta E^{\text{exp}}$ , can be well accounted for by introducing an effective temperature of  $T_{\text{eff}} = \sqrt{T^2 + (\Delta E^{\text{exp}}/4k_B)^2}$  in the FD function (cf. Ref. [19]).
  - [18] J.M. MacLaren *et al.*, *Comput. Phys. Commun.* **60**, 365 (1990).
  - [19] T.J. Kreutz, Ph.D. thesis, University of Zürich, 1997.
  - [20] R.S. Williams, P.S. Wehner, J. Stör, and D.A. Shirley, *Phys. Rev. Lett.* **39**, 302 (1977).
  - [21] The same scattering processes may be relevant also for other phenomena: From spin-resolved photoemission data [A.K. See and L.E. Klebanoff, *Phys. Rev. Lett.* **74**, 1454 (1995)] a  $4sp \rightarrow 3d$  charge transfer in the minority channel was inferred as a mode of core level screening.
  - [22] Thermal effects can account for only about 50% of the line broadening.